Correction

NEUROBIOLOGY. For the article "The SNARE protein SNAP-25 is linked to fast calcium triggering of exocytosis," by Jakob B. Sørensen, Ulf Matti, Shun-Hui Wei, Ralf B. Nehring, Thomas Voets, Uri Ashery, Thomas Binz, Erwin Neher, and Jens Rettig, which appeared in number 3, February 5, 2002, of *Proc. Natl. Acad. Sci. USA* (**99,** 1627–1632), the footnote symbols in the author line appeared incorrectly due to a printer's error. The correct author line and affiliations appear below.

Jakob B. Sørensen*[†], Ulf Matti[‡§], Shun-Hui Wei*[¶], Ralf B. Nehring*, Thomas Voets*[‖], Uri Ashery*,**, Thomas Binz[‡], Erwin Neher*, and Jens Rettig*[§]

*Max-Planck-Institut für Biophysikalische Chemie, Am Fassberg 11, 37077 Göttingen, Germany; [‡]Institut für Physiologische Chemie, Medizinische Hochschule Hannover, 30625 Hannover, Germany; and [§]Physiologisches Institut, Universität des Saarlandes, 66424 Homburg, Germany

The SNARE protein SNAP-25 is linked to fast calcium triggering of exocytosis

Jakob B. Sørensen*†, Ulf Matti‡§, Shun-Hui Wei*¶, Ralf B. Nehring*, Thomas Voets*‖, Uri Ashery*,**, Thomas Binz‡, Erwin Neher*, and Jens Rettig*‡

*Max-Planck-Institut für Biophysikalische Chemie, Am Fassberg 11, 37077 Göttingen, Germany; ‡Institut für Physiologische Chemie, Medizinische Hochschule Hannover, 30625 Hannover, Germany; and §Physiologisches Institut, Universität des Saarlandes, 66424 Homburg, Germany

Synchronous neurotransmission depends on the tight coupling between Ca^{2+} influx and fusion of neurotransmitter-filled vesicles with the plasma membrane. The vesicular soluble *N*-ethylmaleimide-sensitive factor attachment protein receptor (SNARE) protein synaptobrevin 2 and the plasma membrane SNAREs syntaxin 1 and synaptosomal protein of 25 kDa (SNAP-25) are essential for calcium-triggered exocytosis. However, the link between calcium triggering and SNARE function remains elusive. Here we describe mutations in two sites on the surface of the SNARE complex formed by acidic and hydrophilic residues of SNAP-25 and synaptobrevin 2, which were found to coordinate divalent cations in the neuronal SNARE complex crystal structure. By reducing the net charge of the site in SNAP-25 we identify a mutation that interferes with calcium triggering of exocytosis when overexpressed in chromaffin cells. Exocytosis was elicited by photorelease of calcium from a calcium cage and evaluated by using patch-clamp capacitance measurements at millisecond time resolution. We present a method for monitoring the dependence of exocytotic rate upon calcium concentration at the release site and demonstrate that the mutation decreased the steepness of this relationship, indicating that the number of sequential calcium-binding steps preceding exocytosis is reduced by one. We conclude that the SNARE complex is linked directly to calcium triggering of exocytosis, most likely in a complex with auxiliary proteins.

The soluble *N*-ethylmaleimide-sensitive factor attachment protein receptor (SNARE) proteins form the basic machinery needed for fusion of intracellular membrane compartments with each other or the plasma membrane (1–3). Whereas most membrane fusion reactions in the cell are constitutive, neurotransmission relies on the precise timing of release with calcium influx at the release site. This fact raises the question of how SNARE function is coupled to calcium influx. In principle, a calcium sensor for exocytosis could be intrinsic to the SNARE complex, or it could be distinct from it and mediate its effect allosterically. In support of the latter possibility, synaptotagmin I, which contains two calcium- and lipid-binding C2 domains, has been described as a calcium sensor for exocytosis (4, 5). However, several calcium sensors seem to be involved. For instance, in mice lacking synaptotagmin I synchronized release is abolished, but slower asynchronous calcium-dependent release persists (6, 7).

Several observations suggest a role of the SNARE complex in a calcium-dependent step of exocytosis. Block of secretion in cracked-open PC12 cells by botulinum toxin E, which cleaves synaptosomal protein of 25 kDa (SNAP-25) at R180-I181 was found to be rescued by a SNAP-25 peptide but only in the simultaneous presence of Ca^{2+} (8). Treatment of PC12 cells with botulinum toxin A (cleaves SNAP-25 at Q197-R198) inhibited secretion, but the inhibition was overcome partly at higher intracellular Ca^{2+} concentration ($[Ca^{2+}]_i$), a change that was paralleled by a shift in Ca^{2+}-dependent binding of synaptotagmin to SNAP-25 toward higher Ca^{2+} concentrations (9). The interpretation of these studies is complicated by the fact that exocytosis of large dense core vesicles in PC12 cells is 100-fold

slower than in chromaffin cells (10). Therefore PC12 cells most likely lack the biphasic exocytotic burst component, which is characteristic for secretion from chromaffin cells (11, 12) and attains release rates similar to synchronous release in neurons. In the present study we investigated whether mutations on the outside of the SNARE complex would affect the calcium dependence of burst-like large dense core vesicle secretion from chromaffin cells.

Materials and Methods

Plasmid Construction, Mutagenesis, and Overexpression. Green fluorescent protein (GFP)-SNAP-25A was inserted into a modified pSFV1 vector (GIBCO/BRL) as described (13). SNAP-25 mutants were generated by PCR using suitable primers. A plasmid encoding full-length rat synaptobrevin 2 was kindly provided by Dirk Fasshauer (Göttingen, Germany). The cytosolic domain of synaptobrevin 2 was amplified by PCR and inserted into *Nde*I/*Bam*HI-cut vector pET15b (Novagen) or pSP73 (Promega) using its *Xba*I/*Hin*dIII restriction sites. For overexpression of synaptobrevin 2, an internal ribosome entry site from poliovirus followed by enhanced GFP was introduced into the *Sma*I site of the modified pSFV1 vector. The gene coding for full-length synaptobrevin 2 was modified by PCR to generate a Kozak consensus sequence and inserted upstream of the poliovirus internal ribosome entry site by using *Bam*HI and *Bss*HII restriction sites. The nucleotide sequence of all constructs was verified by DNA sequencing.

Overexpression of SNAP-25 mutants and synaptobrevin was evaluated by the green fluorescence of the cells and by Western blot using standard techniques. The primary antibodies used were a kind gift from Reinhard Jahn [MPI für Biophysikalisce Chemie, Göttingen, Germany; mouse anti-SNAP-25, 1:10,000 (Cl 71.2; ref. 14), and mouse anti-synaptobrevin, 1:3,000 (Cl 69.1; ref. 15)]. Western blot of SNAP-25 mutants verified overexpression of full-length SNAP-25-GFP fusion protein but also, not unexpected, the presence of several protein breakdown products. Previous studies showed that overexpression of wild-type SNAP-25-GFP does not modify secretion significantly and that overexpression of a deletion mutant of SNAP-25 with the nine C-terminal amino acids removed led to the identical phenotype as when the nine C-terminal amino acids were cleaved by perfusion with botulinum toxin A (13). Because breakdown

NEUROBIOLOGY

products of SNAP-25-GFP are present to the same extent also under these conditions (data not shown), we conclude that they do not interfere with secretion. Western blot of synaptobrevin-expressing cells showed no detectable breakdown products and >20-fold overexpression over the cells' native synaptobrevin. For measurements, cells were selected based on similar fluorescence levels such that the level of overexpression would not vary between conditions and mutants.

Photolysis of Caged Ca²⁺, Whole-Cell Capacitance, and Ca²⁺ Measurements. Experimental procedures related to flash photolysis were performed as described (11, 13). Nitrophenyl-EGTA was supplied by G. Ellis-Davies (MCP Hahnemann University, Philadelphia).

For calcium ramp experiments (Fig. 4), calcium was measured by using a mixture of 400 μM Fura-4F (Molecular Probes; K_d for calcium, 1 μM), and 400 μM furaptra (Molecular Probes; K_d, 40 μM). The signal (ratio of fluorescence with excitation at 350 and 380 nm) was calibrated *in vivo* by making whole-cell patches with eight different pipette solutions with known calcium concentrations (12). The ramp was elicited by the fluorescence excitation light alternating between 350 and 380 nm at 40 Hz such that photolysis of nitrophenyl-EGTA could be combined with simultaneous measurement of $[Ca^{2+}]_i$. For off-line analysis, the simultaneously obtained capacitance trace was averaged to give one capacitance value per calcium measurement (Fig. 4b, second trace). The rate between two consecutive measurements was calculated as

$$\text{rate}_j = \frac{C_{m,j} - C_{m,j-1}}{\Delta t} \quad j = 2, \dots, N \qquad [1]$$

where $C_{m,j}$ is the averaged capacitance around the jth calcium measurement, and Δt is the time between measurements (Fig. 4b, third trace). To calculate the rate constant, an estimate for the vesicle pool size is required. This estimate is difficult to obtain, because the contributions of individual vesicle pools are not always obvious in ramp experiments. We adopted the technique of numerically differentiating the (raw) capacitance trace and fitting a Gaussian distribution to the (smoothed) derivative to find the time of fastest capacitance increase (the top point of the Gaussian). We assumed that the pool would comprise 2 times the capacitance change up to this point. This method measures the rate constants of the vesicle pool that fuses first, i.e., the pool with the highest rate constant at low $[Ca^{2+}]_i$. For control cells this will be the readily releasable pool; however, some contamination from the slowly releasable pool cannot be excluded. We assume that pool estimates in practice were correct within 20–30%.

By using this estimate, we calculated the remaining pool size (Fig. 4b, fourth trace) corresponding to each rate measurement (pool$_j$) and calculated the rate constant, rc_j (Fig. 4b, fifth trace), as $rc_j = \text{rate}_j/\text{pool}_j$. Finally, the rate constant was plotted as a function of the interpolated $[Ca^{2+}]_i$ between the two measurements, giving rise to the rate estimate (Fig. 4c). The underlying assumption of this plot is that the calcium ramp was slow enough that the calcium sensor can be considered to be in equilibrium with calcium at all times ("quasi steady state"). Simulations of the standard secretory model (Fig. 4f *Upper*) showed that this was the case for the calcium ramps used in this paper.

To bin results from several cells (Fig. 4 d and e), paired results of calcium and rate constants from each cell (see Fig. 4c) were transformed by $(x,y) \rightarrow [\log x, \log(y + 1)]$, where x is $[Ca^{2+}]_i$, and y is the rate constant [transformation of the rate by $\log(y + 1)$ was necessary, because measured rates could be negative]. After binning for calcium on this logarithmic scale, the mean $\pm$ SEM was calculated on transformed data, and the mean and limits were back-transformed to give the plots in Fig. 4 d and e.

Results and Discussion

The Site D58/E170/Q177 in SNAP-25. The neuronal SNARE complex is characterized by a number of charged amino acids pointing toward the outside of the complex, representing possible interaction sites with auxiliary proteins or factors (including calcium; ref. 16). In the present study we asked whether these charges modulate secretion in chromaffin cells. In the selection of putative interaction sites we were led by the description of divalent strontium ions at the surface of the crystallized core complex that are coordinated partly by acidic and hydrophilic amino acid side chains (16, 17). One such site is formed between the two helices of SNAP-25 by the acidic/hydrophilic residues D58, E170, and Q177 (Fig. 1a). To eliminate any putative electrostatic interaction with external factors, we mutated these three amino acids to alanine and overexpressed the resulting mutant as a fusion protein with GFP in bovine chromaffin cells by using the Semliki Forest virus (SFV) system (13, 18). Exocytosis was monitored by measuring the membrane capacitance during whole-cell patch-clamp recording (19) and by simultaneous measurement of oxidation current (amperometry) of the released catecholamines by using a carbon fiber placed next to the cell (20). The cells were loaded with the caged-calcium compound nitrophenyl-EGTA and calcium-sensitive dye(s) by infusion through the pipette. Exocytosis was elicited by applying a strong UV flash to release calcium from nitrophenyl-EGTA, resulting in a step-like increase in $[Ca^{2+}]_i$ (11, 21).

Overexpression of the SNAP-25 mutant D58A/E170A/Q177A caused a dramatic decrease in secretion as monitored by both capacitance change and amperometry (Fig. 1b). Separate circular dichroism spectroscopy and biochemical experiments verified that SNAP-25 D58A/E170A/Q177A forms SDS-resistant complexes with synaptobrevin and syntaxin with unchanged content of secondary structure (data not shown) and a melting temperature comparable to that of wild-type complexes (58.3°C for the mutant, 61.1°C for wild-type complexes in the presence of 2% SDS). Previously, it was shown that overexpression of SNAP-25 in chromaffin cells by the SFV system leads to ≈25-fold overexpression over the native SNAP-25 and that overexpressed wild-type GFP-linked SNAP-25 assembles into SNARE complexes *in vivo* without any deleterious effect on secretion (13). Therefore, the reduction of secretion followed functional replacement of the triple-mutated SNAP-25 into SNARE complexes.

The response to flash photorelease of calcium in control chromaffin cells consists typically of a capacitance increase that follows a triple exponential time course. The fast burst (time constant, $\tau = 20–30$ ms) and slow burst ($\tau = 200–300$ ms) components represent the parallel fusion of two release-ready pools of vesicles, the rapidly and slowly releasable pools, respectively (11, 22), whereas the sustained ($\tau > 1$ s) component represents refilling of the releasable pools from a larger pool of docked but unprimed vesicles (23, 24) followed by fusion. The kinetics were analyzed by scaling the mutant secretion to the control amplitude 1 s after the flash (Fig. 1c) and fitting exponentials to individual responses. The results showed that the mutant response was reduced strongly and that the amplitudes of the rapidly and the slowly releasable pool components were reduced by a similar factor (Fig. 1d), whereas the time constants were unchanged (Fig. 1e).

In an attempt to create a milder phenotype, we investigated the effect of the double mutant SNAP-25 E170A/Q177A, where only one negative charge was eliminated from the interaction site. This mutant also formed SDS-resistant SNARE complexes giving circular dichroism spectra with α-helical structure comparable to its wild-type counterpart (melting temperature 59.9°C; wild-type complex, 61.1°C). Overexpression of this mutant also led to a decrease in secretion (Fig. 1f), but compared
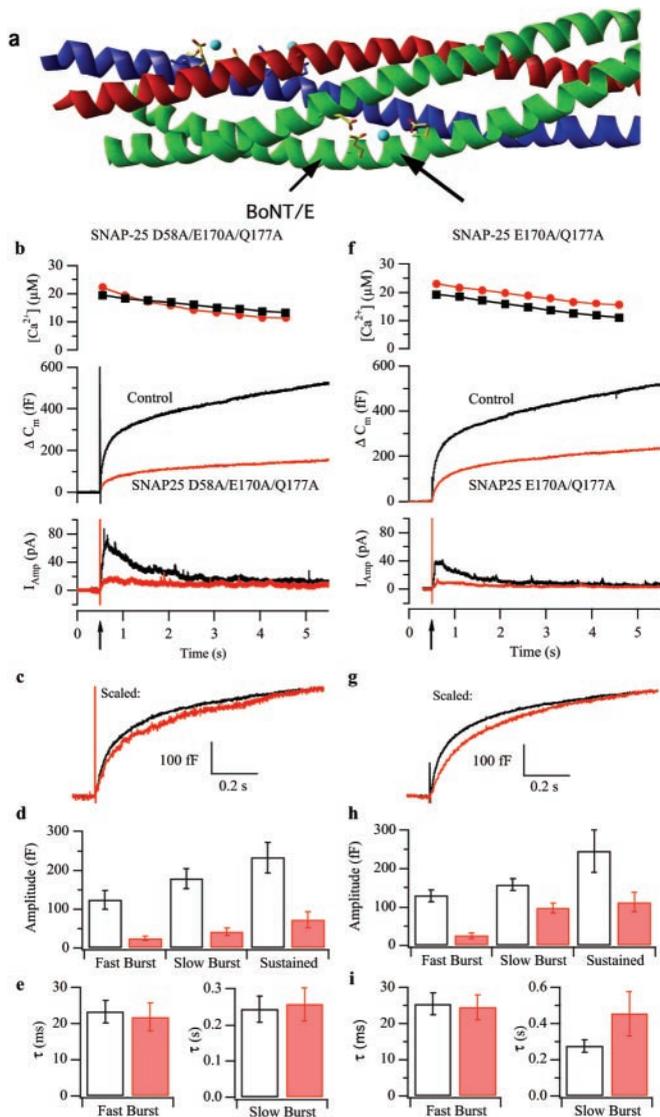
Fig. 1. Mutation in the site D58/E170/Q177 in SNAP-25 inhibits secretion. (*a*) Crystal structure of the core complex. Red, syntaxin 1; blue, synaptobrevin 2; green, SNAP-25; and light blue, strontium ions (16). Membrane anchors (not shown) link to the complex at the left side. Side chains of amino acids interacting with strontium ions are shown as sticks. The arrows point to the site studied in this figure and the botulinum toxin E (BoNT/E) cleavage site. (*b*) Secretion from chromaffin cells after flash photorelease of calcium. Shown are means of 31 control (not expressing) cells (black) and 29 cells overexpressing SNAP-25 D58A/E170A/Q177A (red). (*Top*) [Ca^{2+}]$_i$ after flash photolysis of nitrophenyl-EGTA (arrow on the time scale). Preflash [Ca^{2+}]$_i$ was 200–500 nM. (*Middle*) Mean capacitance change. (*Bottom*) Mean amperometric current. (*c*) Mean capacitance change from mutant cells (red) scaled to the amplitude of control data (black) at 1 s after the flash. (*d* and *e*) Amplitudes and time constants (mean ± SEM) of exponential fits to individual responses. (*f–i*) Double mutation in the site D58/E170/Q177 in SNAP-25 slows down secretion. Means of 47 control cells (black) and 36 cells overexpressing SNAP-25 E170A/Q177A (red) are shown. For explanation, see *b–e* legends.

with the triple mutant more secretion remained. Notably, when scaled to the control amplitude, secretion in the first second after the flash was slower than in control cells (Fig. 1*g*). Exponential fitting revealed that this decrease apparently was caused by a disproportional reduction of the fast burst amplitude (Fig. 1*h*) and an increase in the slow burst time constant (Fig. 1*i*). We conclude that the integrity of the site D58/E170/Q177 in SNAP-25 is critical for exocytosis and that mutation causes
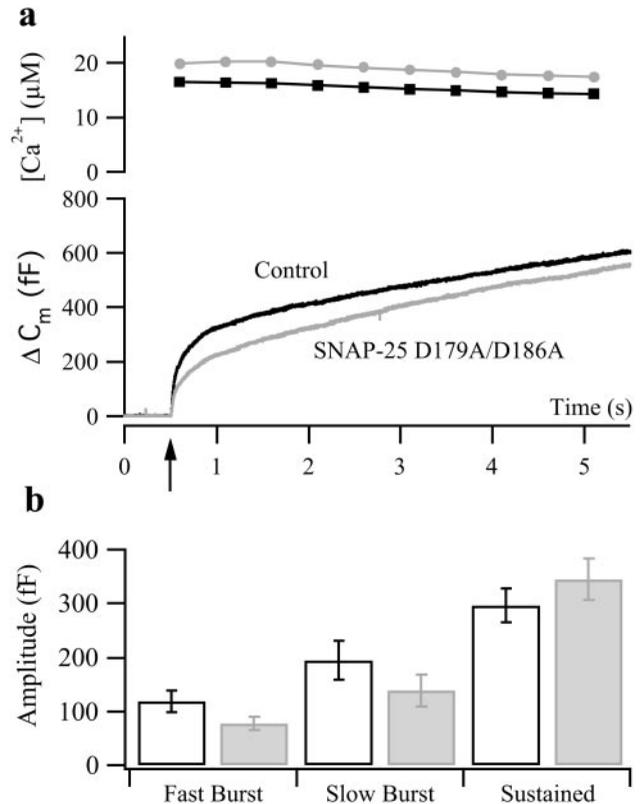

Fig. 2. The double charge-neutralizing mutation D179A/186A in the C-terminal end of SNAP-25 moderately decreases secretion. The means of 33 control cells (black) and 30 cells overexpressing SNAP-25 D179A/186A are shown (gray). For explanation, see Fig. 1 *b* and *d* legends.

substantial decreases in overall secretion, as well as slowdown of the remaining secretion in the double mutant.

Negative Charges in the C-Terminal Domain of SNAP-25. The importance of the C-terminal end of SNAP-25 for exocytosis has been revealed by experiments by using the neurotoxin botulinum toxin E that cleave off the C-terminal end of SNAP-25 and abolishes secretion in chromaffin cells (25). Recent results indicated that a series of negative charges located in the C-terminal end and pointing toward the outside of the complex (D179, E183, D186, D193, and E194) are of particular importance and that progressive neutralization of these charges leads to inhibition of calcium-triggered exocytosis.[††] However, in cracked-open PC12 cells it was found that neutralization of negative charges (especially D186) led to increased rescue of botulinum toxin E-poisoned cells (26). The D58/E170/Q177 site is located N-terminal to this region and thus remains in the bulk of the protein even after botulinum toxin E cleavage. We asked whether the effect seen after removal of negative charges in the D58/E170/Q177 site might be mimicked by neutralization of negative charges in the C-terminal end of SNAP-25. To this end we studied the mutant SNAP-25 D179A/D186A after overexpression in chromaffin cells. Secretion in mutant cells was characterized by a moderate reduction in the burst component of secretion (Fig. 2). Kinetic analysis showed that the reduction was caused by a decrease in the amplitude of both fast and slow burst components (Fig. 2*b*), with their time constants being unaffected (data not shown). These data support a positive role in secretion for the negative

---

[††]Kim-Miller, M. J., Zhang, X., Larsen, E. C., Haberly, L. B., Martin, T. F. (2000) *Neuroscience Meeting 2000*, Nov. 4–9, 2000, p. 128.15 (abstr.).
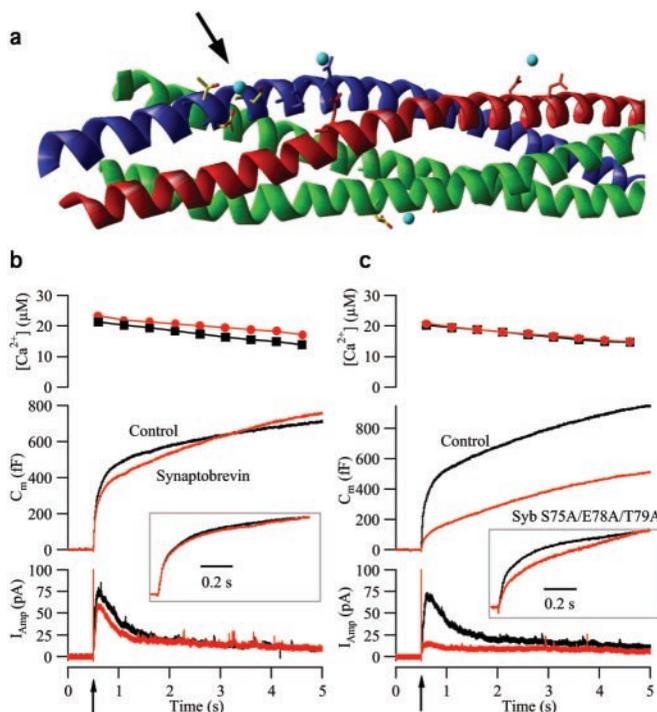
NEUROBIOLOGY

Fig. 3. Triple mutation in the site S75/E78/T79 in synaptobrevin blocks the burst phase of secretion. (*a*) Crystal structure of the core complex. Red, syntaxin 1; blue, synaptobrevin 2; green, SNAP-25; and light blue, strontium ions. The arrow points to the studied site. (*b*) The means of 51 control (not expressing) cells (black) and 35 cells overexpressing synaptobrevin wild type (red). (*Top*) Mean $[Ca^{2+}]_i$ after the flash. (*Middle*) Mean capacitance change. (*Bottom*) Mean amperometric current. (*Inset*) The mean trace from cells overexpressing synaptobrevin wild type scaled to the control data at 1 s after the flash. (*c*) The means of 47 control cells (black) and 42 cells overexpressing synaptobrevin S75A/E78A/T79A (red). Explanation is the same as that for *b*.

amino acids in the C-terminal end of SNAP-25. Still, when considering the overall capacitance change at the end of the measurement (Fig. 2*a*), i.e., 5 s after the flash, it becomes apparent that the D179A/D186A mutation caused a reduction of only 8% compared with the dramatic effect of neutralizing one or two charges in the D58/E170/Q177-binding pocket (Fig. 1 *f* and *b*, reductions by 55 and 71%, respectively). A second flash stimulation applied 2 min after the first revealed a further decrease of secretion in the D179A/D186A mutant [to 58% of the control value (data not shown)] because of a reduction in both fast and slow burst components. This result indicates that this mutation may affect the refilling of the releasable vesicle pools after emptying. We conclude that several negative charges in this part of the protein are involved in exocytosis but that the charges in the D58/E170/Q177 site seem to be of special importance for fast Ca^{2+}-dependent triggering.

The Site S75/E78/T79 in Synaptobrevin. We next asked whether similar effects could be identified when mutating other putative interaction sites. In the SNARE complex crystal structure, another strontium ion is bound between the side chains of S75, E78, and T79 in synaptobrevin (ref. 17; Fig. 3*a*). In the core complex, this site is located in close proximity to the cleavage site for botulinum toxin A in SNAP-25; thus it is closer to the membrane anchors than the D58/E170/Q177 site in SNAP-25, and it was speculated that it might modulate the calcium dependence of exocytosis (17).

We mutated all three interacting amino acids to alanines and expressed the resulting synaptobrevin S75A/E78A/T79A mu-

tant in chromaffin cells together with GFP. We verified that the S75A/E78A/T79A synaptobrevin mutant formed SDS-resistant complexes with its partners (melting temperature 65.4°C; wild-type complex, 61.1°C) showing no detectable changes in the SNARE complex structure as judged by circular dichroism spectroscopy. As a control we also studied overexpression of synaptobrevin wild type, because this had not been tested thus far in chromaffin cells. Overexpression of synaptobrevin wild type led to only small changes in secretion (Fig. 3*b*), and the amount of overall secretion after 5 s was unchanged. After scaling of the exocytotic burst, the control and synaptobrevin wild-type traces overlapped almost perfectly (Fig. 3*b Inset*), indicating that the kinetic properties of the burst were unchanged. In contrast, overexpression of the synaptobrevin S75A/E78A/T79A mutant led to a dramatic reduction of secretion (Fig. 3*c*) characterized by a large reduction in burst but an unchanged sustained component. Scaling showed that the capacitance change was slowed down compared with control cells (Fig. 3*c Inset*), although the retarded component was preceded by a faster part, unlike the slowdown of the SNAP-25 E170A/Q177A (compare Figs. 3*c* and 1*g*). From these experiments we conclude that the S75/E78/T79 site in synaptobrevin is important for secretion, with its main effect being to decrease the size of the exocytotic burst, whereas the recruitment after high calcium stimulation is hardly affected.

The Calcium Dependence of Secretion at Low Calcium Concentrations. If the calcium sensor for exocytosis is either linked to the SNARE complex or integral to it, mutation in the SNARE complex may alter the calcium dependence of secretion. To address this question, we devised a method to derive the dependence of the secretory rate constant on $[Ca^{2+}]_i$ at the release site. The ideal calcium concentration for these studies is 0.5–5 μM, because in this concentration range the calcium sensor is expected to be far from saturation. At the same time, the limitation of being able to give only two or three stimulations to a single cell (due to run-down) combined with significant cell-to-cell variability made it advantageous to derive the entire calcium dependence from a single stimulation.

The solution was to use a calcium ramp technique where calcium was liberated slowly from the calcium cage over the course of 2–5 s by weak UV illumination. The UV illumination was alternated between 350 and 380 nm, allowing the simultaneous fluorimetric measurement of $[Ca^{2+}]_i$. In the control cell shown in Fig. 4*a*, a calcium ramp triggered a faster phase of capacitance increase followed by a slower, more sustained phase. Data analysis was carried out as shown in Fig. 4*b*. Based on a calculation of the local rate of capacitance change around each calcium measurement and an estimate of the size of the releasable pool (Fig. 4*a*), the rate constant was calculated around each calcium measurement. The rate constant then was replotted as a function of the $[Ca^{2+}]_i$, yielding the desired relationship (Fig. 4*c*).

Fig. 4 *d* and *e* show plots of rate constants versus $[Ca^{2+}]_i$ obtained from several cells. From Fig. 4*d* it is evident that for low calcium concentrations (0.5–2 μM), control cells displayed a steeper relationship of the rate constant on $[Ca^{2+}]_i$ than cells overexpressing the SNAP-25 E170A/Q177A mutants. The slope was 2.7 for the control and 1.5 for the mutant cells. This result already indicates a difference in the number of calcium ions involved in exocytosis. To achieve a more precise description, we fitted the relationships in Fig. 4*d* with sequential calcium-binding models for exocytosis (Fig. 4*f*). The simplest possible such model assumes that calcium binds sequentially and noncooperatively to three similar binding sites on the calcium sensor for exocytosis to occur (12). A satisfactory fit of this model to mean control data (upper blue line in Fig. 4*d*) was obtained with only minor changes compared with the previously published values (ref. 12;
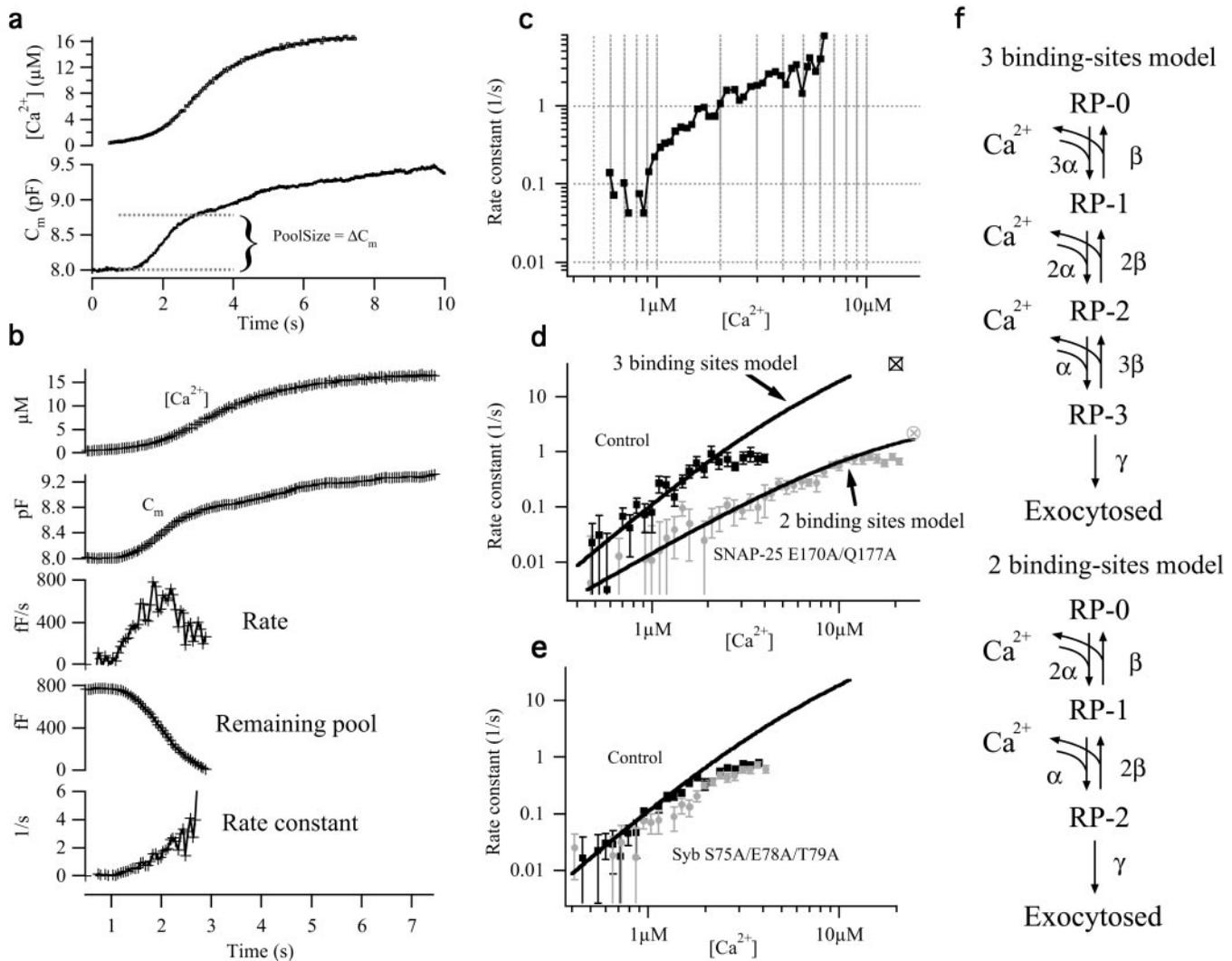
Fig. 4. Double mutation in the D58/E170/Q177 site changes the calcium dependence of exocytosis. (*a*) Example of a control cell stimulated by continuous weak UV illumination. Capacitance (line, *Bottom*) and calcium (small boxes, *Top*) measurements are shown. (*b*) Rate constant calculations. The capacitance trace was averaged (second trace) around each calcium measurement (first trace), and the local rate was calculated (third trace). Based on an estimate of the size of the readily releasable pool (see *a*), the remaining pool size was calculated (fourth trace), and finally the rate constant (fifth trace) was calculated as the rate divided by remaining pool size. (*c*) Plot of rate constant versus $[Ca^{2+}]_i$ on a double logarithmic scale. (*d*) Double logarithmic plot of rate constant versus calcium for 15 control cells (black squares) and 13 cells overexpressing the SNAP-25 E170A/Q177A mutant (gray circles). For comparison with ramp data, the rates for the corresponding flash data (from fig. 1*i*) are indicated with open symbols with crosses. For the control cells the rate for the readily releasable pool was taken, and for the mutant cells the rate for the slowly releasable pool was chosen. The flash rates confirm that the apparent saturation of ramp rates at around 1 s is artificial, probably caused by some contamination of the pool size estimate with slower components at later times. Fitted to control data are the three binding-sites secretory model in *f*, whereas fit to mutant data are the two binding-sites model. (*e*) Double logarithmic plot of rate constant versus calcium for 13 control cells (black squares) and 13 cells overexpressing the synaptobrevin S75A/E78A/T79A mutant (gray circles). The line is the same fit of the three-step model as the one in *a*. (*f*) Sequential calcium-binding models for exocytosis. (*Upper*) Standard model for chromaffin cells, with three equivalent calcium-binding sites. (*Lower*) Modified model, with only two equivalent calcium-binding sites. The models were solved numerically by using a fourth order Runge-Kutta method with automatic step-size control and a typical calcium ramp as forcing function. A simplex method was used to fit the models to the estimated data in *d*. Fitted parameters in the three binding-sites model (fit to controls in *d*; only α was varied, β and γ were taken from ref. 12): $\alpha = 5.7\ \mu M^{-1} \cdot s^{-1}$; $\beta = 56\ s^{-1}$; and $\gamma = 1450\ s^{-1}$. Fitted parameters in the two binding-sites model (fit to SNAP-25 E170/177A data): $\alpha = 4.2\ \mu M^{-1} \cdot s^{-1}$; $\beta = 69\ s^{-1}$; and $\gamma = 4.7\ s^{-1}$.

$\alpha = 5.7\ \mu M^{-1} \cdot s^{-1}$ instead of $4.4\ \mu M^{-1} \cdot s^{-1}$). In contrast, to fit the shallower slope of the SNAP-25 E170A/Q177A relationship, the number of calcium-binding sites in the model was reduced by one (Fig. 4*f Lower*). With this change, then, the model showed a satisfactory fit to the mutant data (Fig. 4*d*, lower blue line) by assuming a much lower maximal rate ($\gamma = 4.7\ s^{-1}$ instead of $1,450\ s^{-1}$ for the controls) but in the absence of large changes in on- or off-rates for calcium (see Fig. 4 legend). This is the expected result if a binding site for calcium had been eliminated by the mutation and simultaneously it had been made possible for vesicles to fuse by using the two remaining binding sites.

The corresponding calcium ramp measurements on the synaptobrevin S75A/E78A/T79A mutant showed that the slope in the double logarithmic plot was almost unchanged (Fig. 4*e*), although the rates for the mutants were on average a little lower than in control cells. Therefore, we conclude that although mutation of the S75/E78/T79 site leads to a depression in secretion (Fig. 3), the fastest part of the remaining secretion (which is the part that in effect is analyzed in calcium ramp experiments, see *Materials and Methods*) exhibits an almost unchanged dependence on $[Ca^{2+}]_i$. The integrity of the S75/E78/T79 site therefore is important for maintaining the size of

NEUROBIOLOGY

primed vesicle pools before stimulation, but apparently it does not modulate Ca^{2+}-dependent triggering.

In Fig. 4d we compared the rate data obtained by the ramp method with the rates obtained at higher $[Ca^{2+}]_i$ values by flash experiments (symbols with crosses) using the rapidly releasable pool rate for the control situation and the slowly releasable pool rate for the E170A/Q177A mutant (Fig. 1i). These rates fall on the extension of the model fits to higher calcium values. This result validates the ramp method and also indicates that in effect the measured rate for the E170A/Q177A mutant is that of the slowly releasable pool, because the rapidly releasable pool in this case is too small to be resolved in ramp experiments. It is an open question whether the slowly releasable pool in E170A/Q177A-expressing cells has the same molecular basis as the slowly releasable pool in control cells, but if this was the case, it would mean that the slow release from the slowly releasable pool can be viewed as being that of a rudimentary fusion machine, characterized by a shallower calcium dependence.

Because mutation in the D58/E170/Q177 binding pocket abolished one calcium-binding site in the calcium sensor for exocytosis, apparently this site interacts with or constitutes part of the calcium sensor for exocytosis. There are two possible ways in which this could come about. First, the D58/E170/Q177 site could interact directly with calcium. Because the site does not provide the full coordination sphere required for calcium binding, simultaneous binding of another protein such as synaptotagmin I would be necessary to generate a full calcium-binding site. The other possibility is that the D58/E170/Q177 site could bind to another protein, which then in turn could bind calcium. The "rudimentary fusion machine" discussed above might represent a SNARE complex without such a protein bound. If calcium was to bind directly and exert an electrostatic effect, charge reversals in the pocket might simulate the calcium-bound state and create a functional SNAP-25 mutant. However, charge-reversal mutations (D58K, E170K, and D58K/E170K were studied) eliminated the burst component of secretion (Fig. 5, which is published as supporting information on the PNAS web site, www.pnas.org), and spontaneous fusion was not observed. This is the expected result if the site binds a calcium sensor distinct from the core complex. However, we cannot rule out that SNAP-25 creates a calcium-binding site in a complex with another, unknown partner and that the detailed structural integrity of this binding site is critical for exocytosis to occur.

In conclusion, charged putative binding sites on the outside of the SNARE complex are essential for normal fast calcium-triggered secretion as measured with high time-resolution techniques. Mutation of these sites hardly affects complex stability but has a profound effect on secretion, probably because of loss of an interaction with auxiliary factors/proteins. The finding of a mutant with a reduced calcium dependence of the exocytotic rate means that the calcium sensor of exocytosis is linked intimately to SNARE complex function. The SNARE complex and the calcium sensor therefore constitute parts of an integrated fusion machine.

1. Söllner, T., Whitehart, S. W., Brunner, M., Erdjument-Bromage, H., Geromanos, S., Tempst, P. & Rothman, J. E. (1993) *Nature (London)* **362,** 318–324.
2. Jahn, J. & Südhof, T. C. (1999) *Annu. Rev. Biochem.* **68,** 863–911.
3. Lin, R. C. & Scheller, R. H. (2000) *Annu. Rev. Cell Dev. Biol.* **16,** 19–49.
4. Brose, N., Petrenko, A. G., Südhof, T. C. & Jahn, R. (1992) *Science* **256,** 1021–1025.
5. Fernandez-Chacon, R., Königstorfer, A., Gerber, S. H., Garcia, J., Matos, M. F., Stevens, C. F., Brose, N., Rizo, J., Rosenmund, C. & Südhof, T. C. (2001) *Nature (London)* **410,** 41–49.
6. Geppert, M., Goda, Y., Hammer, R. E., Li, C., Rosahl, T. W., Stevens, C. F. & Südhof, T. C. (1994) *Cell* **79,** 717–727.
7. Voets, T., Moser, T., Lund, P.-E., Chow, R. H., Geppert, M., Südhof, T. C. & Neher, E. (2001) *Proc. Natl. Acad. Sci.* **98,** 11680–11685.
8. Chen, Y. A., Scales, S. J., Patel, S. M., Doung, Y.-C. & Scheller, R. H. (1999) *Cell* **97,** 165–174.
9. Gerona, R. R. L., Larsen, E. C., Kowalchyk, J. A. & Martin, T. F. J. (2000) *J. Biol. Chem.* **275,** 6328–6336.
10. Kasai, H. (1999) *Trends Neurosci.* **22,** 88–93.
11. Heinemann, C., Chow, R. C., Neher, E. & Zucker, R. S. (1994) *Biophys. J.* **67,** 2546–2557.
12. Voets, T. (2000) *Neuron* **28,** 537–545.
13. Wei, S., Xu, T., Ashery, U., Kollewe, A., Matti, U., Antonin, W., Rettig, J. & Neher, E. (2000) *EMBO J.* **19,** 1279–1289.
14. Bruns, D., Engers, S., Yang, C., Ossig, R., Jeromin, A. & Jahn, R. (1997) *J. Neurosci.* **17,** 1898–1910.
15. Edelmann, L., Hanson, P. I., Chapman, E. R. & Jahn, R. (1995) *EMBO J.* **14,** 224–231.
16. Sutton, R. B., Fasshauer, D., Jahn, R. & Brunger, A. T. (1998) *Nature (London)* **395,** 347–353.
17. Fasshauer, D., Sutton, R. B., Brunger, A. & Jahn, R. (1998) *Proc. Natl. Acad. Sci. USA* **95,** 15781–15786.
18. Ashery, U., Betz, A., Xu, T., Brose, N. & Rettig, J. (1999) *Eur. J. Cell Biol.* **78,** 525–532.
19. Neher, E. & Marty, A. (1982) *Proc. Natl. Acad. Sci. USA* **79,** 6712–6716.
20. Leszczyszyn, D. J., Jankowski, J. A., Viveros, O. H., Diliberto, E. J., Jr., Near, J. A. & Wightman, R. M. (1990) *J. Biol. Chem* **265,** 14736–14737.
21. Thomas, P., Wong, J. G. & Almers, W. (1993) *EMBO J.* **12,** 303–306.
22. Voets, T., Neher, E. & Moser, T. (1999) *Neuron* **23,** 607–615.
23. Parsons, T. D., Coorssen, J. R., Horstmann, H. & Almers, W. (1995) *Neuron* **15,** 1085–1096.
24. Ashery, U., Varoqueaux, F., Voets, T., Betz, A., Thakur, P., Koch, H., Neher, E., Brose, N. & Rettig, J. (2000) *EMBO J.* **19,** 3586–3596.
25. Xu, T., Binz, T., Niemann, H. & Neher, E. (1998) *Nat. Neurosci.* **1,** 192–200.
26. Chen, Y. A., Scales, S. J., Jagath, J. R., Scheller, R. H. (2001) *J. Biol. Chem.* **276,** 28503–28508.